APL Materials

Solar thermophotovoltaics: Progress, challenges, and opportunities

Cite as: APL Mater. **7**, 080906 (2019); https://doi.org/10.1063/1.5114829
Submitted: 11 June 2019 . Accepted: 06 August 2019 . Published Online: 26 August 2019

Yang Wang, Haizhou Liu, and Jia Zhu

Solar thermophotovoltaics: Progress, challenges, and opportunities

Cite as: APL Mater. 7, 080906 (2019); doi: 10.1063/1.5114829
Submitted: 11 June 2019 • Accepted: 6 August 2019 •
Published Online: 26 August 2019

View Online Export Citation CrossMark

Yang Wang, Haizhou Liu, and Jia Zhu[a)]

AFFILIATIONS

National Laboratory of Solid State Microstructures, College of Engineering and Applied Sciences, Jiangsu Key Laboratory of Artificial Functional Materials, Nanjing University, Nanjing 210093, People's Republic of China

[a)]Email: jiazhu@nju.edu.cn

ABSTRACT

Solar thermophotovoltaics (STPV), which utilizes the full spectrum of solar energy, possesses a high theoretical system efficiency of 85.4% that well beats the Shockley-Queisser limit of traditional photovoltaics. However, the experimental efficiency reported so far is still less than 10% due to a variety of optical and/or thermal losses. Based on the system efficiency analysis, we first summarize the key components of ideal STPV, which can be divided into the material/structure level and system level. We then introduce new types of solar powered thermophotovoltaics and hybrid STPV systems integrated with other energy conversion systems. A perspective is provided at the end to discuss the challenges and opportunities.

I. INTRODUCTION

The sun is the predominant power source of the solar system, and its radiation power to the earth in 1 h outweighs a year's energy consumption of the human society. However, the direct utilization of solar energy is very limited due to low energy conversion efficiency. In solar cells, for example, the Shockley-Queisser limit is well-known as a theoretical upper limit.[1,2] The low conversion efficiency is rooted in the broadband nature of the solar spectrum, which ranges mostly from 200 nm to 2500 nm. Incident photons with energy lower than the bandgap of the cell cannot be absorbed, while for photons with energy higher than the bandgap, high energy electrons will fall to the edge of the band, with extra energy lost such as heat. The two effects together result in 31% upper limit for single junction solar cell efficiency with no concentration of sunlight, and 41% with maximum solar concentration.[3] Solar thermophotovoltaics (STPV) is an efficient solar energy transfer technology with a potential to exceed the Shockley-Queisser limit, by absorbing sunlight in the entire solar spectrum, and emitting narrowband infrared radiation to PV cells.

Figure 1(a) shows a simplified diagram for the STPV system. Under the idealistic premise of a perfect energy transmission from the absorber to the emitter, the entire energy conversion process can be decomposed into two parts. The first one comprises of the interaction between the sun and the absorber, featured by the blackbody radiation of the two components. The second part is the energy transfer between the emitter and PV cell, the upper limit of which is governed by the Carnot efficiency.[4] The total efficiency η of the system therefore reads

$$\eta = (1 - T^4/T_s^4) \cdot (1 - T_e/T), \tag{1}$$

where T, T_s, and T_e are the temperatures of the absorber, emitter, and sun and PV cell, respectively. Figure 1(b) plots the diagram of Eq. (1), demonstrating a maximum efficiency of 85.4% at 2544 K.

In practice, it is hard to reach the temperature of maximum efficiency as high as 2544 K. As a matter of fact, the conduction and convection of air, as well as the conduction of the sample holder, induces a huge heat loss from the absorber and emitter surfaces, resulting in a low operating temperature. Fortunately, 70% efficiency can be achieved at a moderate temperature of 1000 K, which is nearly twice of the Shockley-Queisser limit. Despite the high temperature requirements for the absorber and emitter, the PV cell needs to be kept cool to maintain a high performance. When the temperature rises, both the efficiency and power of the cell decrease (0.4%–0.5%/K for silicon solar cells).[5] Besides, various optically qualified materials are prone to oxidization at high-temperature, leading to the necessity for a vacuum or inertia environment.

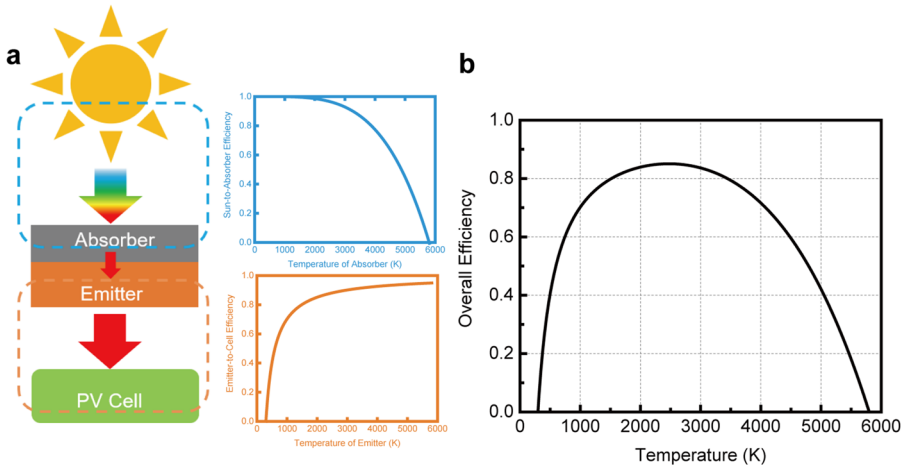

FIG. 1. Solar thermophotovoltaic system. (a) Schematic of a typical STPV configuration. The sun-to-absorber and emitter-to-cell efficiency is, respectively, sketched in blue and orange. (b) The overall efficiency of an ideal STPV system. The sun and the PV cell are, respectively, modeled as 6000 K and 300 K blackbodies.[4]

The temperature control of the absorber, emitter, and PV cell ensures that they can efficiently operate at their best conditions. Moreover, a high system efficiency also requires efficient radiation transfer. To achieve the highest system efficiency, the absorber should only exchange photons with the sun.[6] This indicates that we should concentrate the sunlight to its maximum concentration of 46 050, which is determined by the diameter of the sun and the distance from the sun to the earth (meanwhile, high concentration is also a pathway to raising the temperature of the absorber and emitter). In practice, multilenses are widely adopted instead of a single lens, as the latter usually fails to achieve extremely high solar concentration and frequently suffers astigmatism and dispersion. Different from the concentrated sunlight, the radiation of the emitter is diffused, which increases the difficulty of oriented energy transmission. One solution is to physically place the cell closely to the emitter, usually hundreds of microns. This straightforward solution, nevertheless, imposes a lot of pressure on the cooling system of the cell.

The Carnot efficiency term in Eq. (1) implies that the emission spectrum of the emitter must be of an extremely narrow band, and the emission peak has to match the bandgap of the PV cell. Some previous works reported narrow-band emitters based on metamaterials or photonic crystal structures.[7–9] However, these designs normally incorporate multiple materials or complex nanostructures that lead to fragility at high temperature. Materials naturally have different expansion coefficients with the temperature change, the discrepancy of which may lead to the collapse of the structure. Nanoscale structures also tend to suffer more from lower melting temperature compared with bulk materials.

In conclusion to this part, two key components are vital to a satisfying performance of the STPV system: temperature control of the absorber/emitter/PV cell system and efficient radiation transportation. A high temperature of the absorber and emitter is required for high system efficiency, and the low temperature of PV cell ensures its good performance. Efficient radiation transportation can be realized by the integration of three elements: high solar concentration which leads to low radiation loss of absorber, radiation escape problem of the emitter to cell, and a narrow-band emission of the emitter which is the key to breaking the Shockley-Quiesser limit.

II. ABSORBERS

A. Blackbody or selective?

Solar absorbers are widely used in multiple solar energy applications such as solar steam[10,11] generations and solar thermoelectric[12] conversion. To enhance the energy conversion efficiency, spectrum selective absorbers have been extensively explored to suppress self-radiation loss of the absorber.[13–17] The spectrum of the sun and the absorber reside in different wavelength ranges, empowering the absorbers with both high solar absorption and low thermal radiation. Selective absorbers are particularly useful under low concentration as the self-radiation intensity is comparable with the solar energy. In STPV systems, actually, the solar concentration appears so high that sometimes little benefit is expected by employing a selective absorber.

As an illustration, we have plotted the 1273 K blackbody radiation spectrum and the solar spectrum with concentrations of 20 suns and 1000 suns (Fig. 2). When the solar concentration approaches 1000, the self-radiation of the absorber is negligible as compared with the solar spectrum, which makes blackbody absorbers a better choice instead. Wang *et al.* calculated the thermal transfer efficiency (η_a) of blackbody absorbers and selective absorbers, as a function of solar concentration and the temperature of the absorber,[18] which reads

$$\eta_a = \frac{C\int \alpha(\lambda)E_{solar}(\lambda)d\lambda - \int \alpha(\lambda)E_B(\lambda,T)d\lambda}{C\int E_{solar}(\lambda)d\lambda}. \quad (2)$$

The results are plotted in Fig. 3. As a selective absorber efficiently suppresses radiation loss, it performs better in the regime with low concentration and high operating temperature (top left area in the diagrams). In the regime featured by high solar concentration and low operating temperature (down right), the blackbody absorber proves better in performance, since the long-wavelength solar irradiation prevails as opposed to thermal radiation.

However, despite their respective prevailing regimes as illustrated above, both blackbody absorbers and selective absorbers are capable of achieving a high transfer efficiency. For a fixed operating temperature, it is true that the former prefers a higher solar concentration, while the latter requires lower solar concentration. Yet,

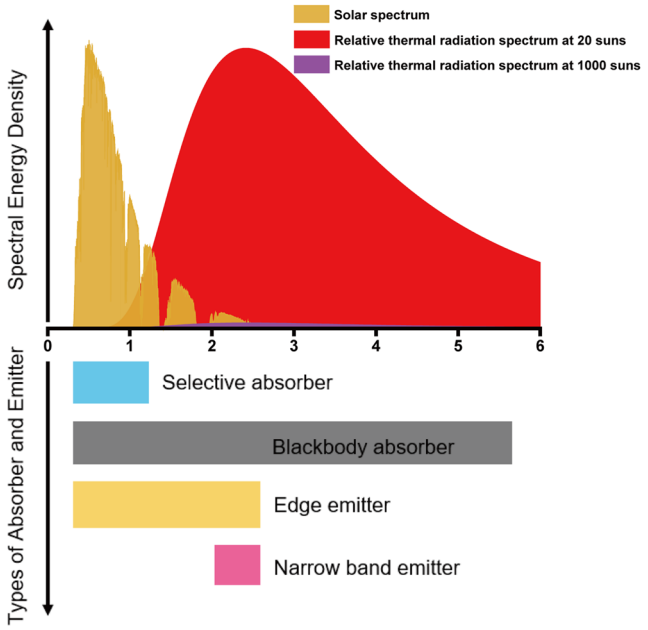

FIG. 2. Spectra and different types of absorbers and emitters, including selective absorbers, blackbody absorbers, edge emitters, and narrow band emitters. The colors indicate the absorption/emission bands of the absorbers/emitters.

they may yield similar thermal transfer efficiency given that the best operating conditions are achieved. This is experimentally proven by Lenert *et al.*[19] and Rinnerbauer *et al.*[20] A similar system efficiency level is achieved by two distinctive input energy levels with the same experiment setup. An input of 780 suns is supplied for the blackbody absorber with a system efficiency of 3.2%,[19] and 180 suns for the selective absorber with 3.74%.[20] A pattern emerges from the experiments and theoretical analysis that the blackbody absorber would be viewed as a better choice when the solar concentration approaches or exceeds 1000 suns; otherwise, a selective absorber is preferred. The above results could also be understood as advantages of the selective absorber, in a way that it enables a lower solar energy input at the same absorber temperature as compared with the blackbody absorber.

B. Nonideal band edges of selective absorber

The performance of selective absorbers depends not only on high absorption in the visible region and low emission in the infrared region but also on the bandwidth of the transition region between the high absorption band and the low emission band [Fig. 4(a)]. As the operating temperature elevates, energy loss due to the spectral overlap between the concentrated solar spectrum and the radiation spectrum becomes significant. A sharp absorption cutoff is therefore important for high-temperature solar absorbers. Most absorber designs, however, have a large cutoff width (longer than 1 μm), which severely compromises the efficiency. Wang *et al.* illustrated a ~20% efficiency drop when the transition bandwidth increases from 0 to 2 μm [Fig. 4(b)].[18] Attributable to the natural selectivity of the semiconductors, the authors demonstrated an extremely sharp absorption cutoff (transition bandwidth ~200 nm), utilizing silicon nanowire arrays as selective absorbers.

C. Current absorbers in STPV systems

Despite the fact that myriads of blackbody and selective solar absorber designs have been discussed in the past 10 years,[13,14,17,21,22] merely a handful of them were proven to contribute to a high performance STPV system. Early works that demonstrated absorbers mainly highlighted their thermal stability, such as high-melting-temperature ceramics and metals. Datas and Algora established an STPV device which uses HfO_2 coated tungsten as the solar absorber and also an infrared emitter,[23] yielding a 0.8% system efficiency. The low efficiency is mainly due to three reasons, namely, high cell temperature, high optical loss in concentration, and unideal optical performance of the absorber and emitter. In order to deal with these drawbacks, in 2014, Lenert and his co-workers first established a nanophotonic STPV device and witnessed a 3.2% system efficiency.[19] They fabricated a multiwalled carbon nanotube as a blackbody absorber which has nearly perfect absorption along the whole solar spectrum [Figs. 5(a) and 5(b)]. The multiwalled carbon nanotube is of a single element and showcases a high temperature tolerance. Soon afterward, a selective absorber with a two-dimensional photonic crystal on a refractory metal is applied on the same device, exhibiting a 3.74% overall efficiency.[20] Circular pits are periodically distributed on reflective Ta in this specific configuration and coated with a HfO_2 layer as an antireflection structure in the visible region [Fig. 5(e)]. This selective absorber greatly reduces the demand for high concentrations of the input solar

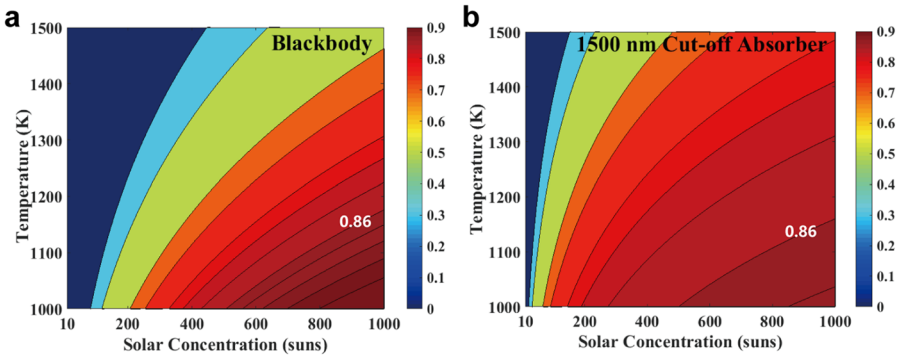

FIG. 3. Thermal transfer efficiency of (a) blackbody absorber and (b) selective absorber. Reprinted with permission from Wang *et al.*, Appl. Phys. Lett. **110**(20), 201108 (2017). Copyright 2017 AIP Publishing LLC.

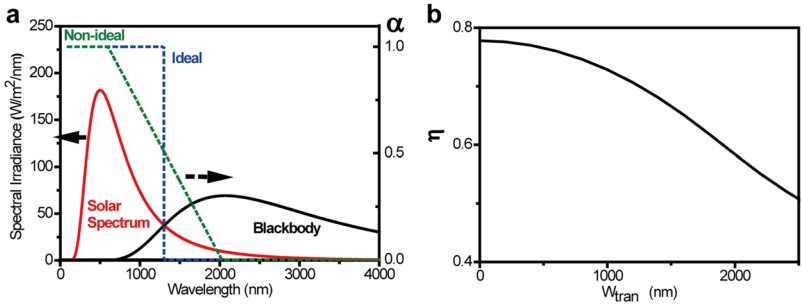

FIG. 4. Band edges of selective absorbers. (a) Ideal (blue) and nonideal (red) bandwidths of the transition region between the high absorption band and the low emission band. (b) The dependence of thermal transfer efficiency on the bandwidth. Reprinted with permission from Wang *et al.*, Appl. Phys. Lett. **110**(20), 201108 (2017). Copyright 2017 AIP Publishing LLC.

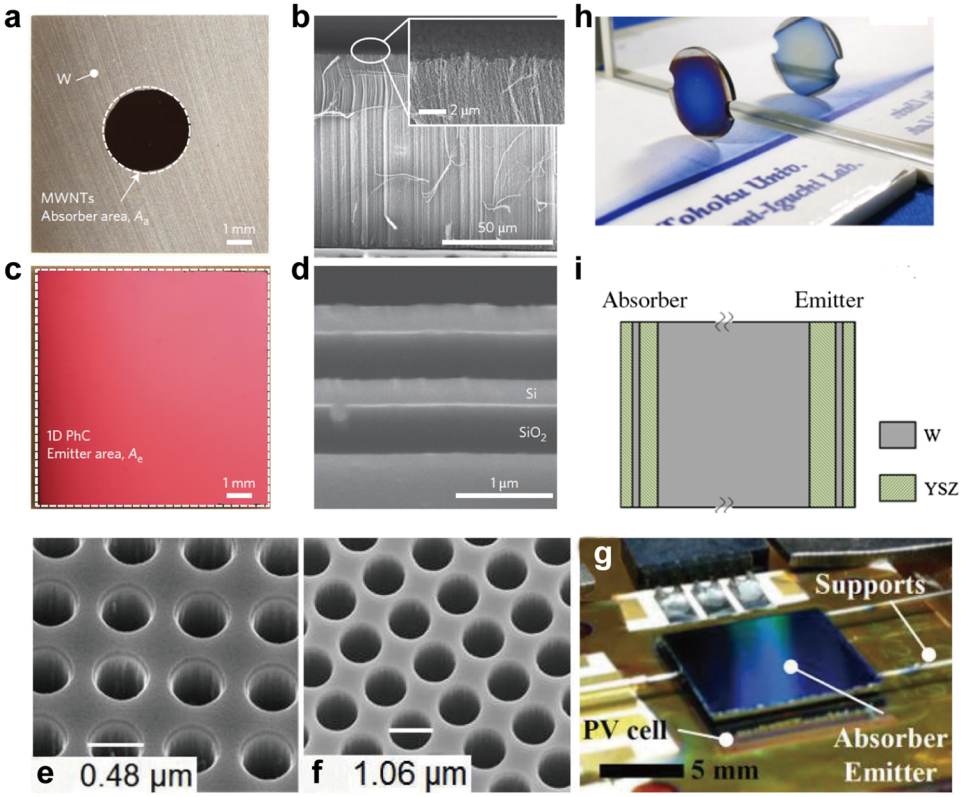

FIG. 5. Absorbers and emitters applied in recent STPV experiments. Devices by Lenert *et al.*: (a) and (b) multiwalled carbon nanotube absorber, (c) and (d) Si/SiO_2 multilayer emitter. Devices by Rinnerbauer *et al.*: (e) tantalum photonic crystal absorber, (f) tantalum photonic crystal emitter, and (g) photography of the absorber and emitter. Devices by Shimizu *et al.*: (h) photograp of the absorber and emitter made from tungsten and yttria-stabilized zirconia, (i) schematic of the absorber and emitter. [(a)–(d)] Reprinted with permission from Lenert *et al.*, Nat. Nanotechnol. **9**(2), 126–130 (2014). Copyright 2014 Springer Nature; [(e)–(g)] Rinnerbauer *et al.*, Adv. Energy Mater. **4**(12), 1400334 (2014). Copyright 2014 WILEY-VCH; and [(h) and (i)] Shimizu *et al.*, J. Photonics Energy **5**(1), 053099 (2015). Copyright 2015 SPIE.

irradiance. In 2015, Shimizu and his co-workers also designed a selective absorber for STPV application;[24,25] a three-layer structure fabricated with refractory metals and dielectric materials [Figs. 5(h) and 5(i)]. Coherent absorption in the thin film results in a wide absorption spectrum in the visible regime. Although other more intricate absorber designs are reported, it is clear that simpler structures with less fancy materials or configurations are favorable for such rigorous high-temperature conditions.

III. EMITTERS

A. Edge emitters and narrowband emitters in STPV systems

Some of the absorber designs can also be applied in thermal emitters by slightly tuning the structural parameters, as the Kirchhoff's law of thermal radiation indicates the equivalence of the absorptivity and emissivity. Currently, two categories of thermal emitters have emerged in the field of STPV (Fig. 2), absorptivity with a step-function (edge emitter) and absorptivity with a narrow band (narrow band emitter). The concrete choice is highly dependent on the internal quantum efficiency (IQE) of the PV cell. To achieve a high emitter-to-cell efficiency, the emission spectrum should match the high IQE part of the cell. In most cases, however, only photons with band-edge energy give the best performance, which means narrow-band emitters are clearly preferable.

It should be noted that, though, edge emitters are still applied in most STPV experiments. This is probably because narrowband emission leads to a large power density decrease, whereas the gain in efficiency is not high enough to compensate. In 2011, Bauer established a model to discuss the impact of the above-bandgap and

sub-bandgap emission on the system efficiency.[26] To evaluate the effect of the emission bandwidth, he introduced concepts as such the sub-bandgap and above-bandgap suppression coefficients into his model. The results did indicate, much within our expectation, that both above-bandgap and sub-bandgap suppression can enhance the system efficiency; however, the former affects little as compared with the latter. Meanwhile, the power density decreases dramatically with the narrow bandgap emission. It can be concluded that the efficiency cannot be considerably improved through additional above-bandgap suppression. Therefore, sub-bandgap suppression is of the top priority in system designs, as is demonstrated in most reported works.

In the experimental setup, Lenert *et al.* fabricated a Si/SiO_2 multilayer emitter with a 1000 nm bandwidth.[19] The multilayer structure is fabricated with low-pressure and plasma-enhanced chemical vapor [Figs. 5(c) and 5(d)] and is annealed after each deposition to enhance its thermal stability. The multilayer structure has a strong interference effect which leads to a step-function-like emission spectrum, although the emissivity varies as the emission angle changes. Two-dimensional photonic crystals are fabricated above refractory metals as edge emitters by Rinnerbauer *et al.*[20] This design is simple in terms of both materials and the structure, ensuring its stability in STPV [Fig. 5(f)]. Furthermore, multiple attempts at constructing narrowband emitters are fabricated via metasurface designs,[7,9] but their real applicability at high temperatures is still in doubt since gold was adopted in the structures.

B. Deviations from unity/zero emittance and optical improvement by filters

Ideally, to achieve high system efficiency, both the absorbers and emitters should reach unity in absorptivity at target wavelengths, which is challenging in the actual experimental setup. To bridge the gap between the theoretical prediction and experimental results, Lenert *et al.* discussed the role of possible spectral nonidealities of absorbers and emitters.[27] They simplified the model by defining deviations from unity/zero emittance above/below the cutoff [Fig. 6(a)]. Systems with lower nonidealities can reach relatively higher efficiency at more moderate solar concentration. Furthermore, wavelength regions with the highest spectral flux dominate the deviation in efficiency, due to the nonuniformity of the radiation spectrum. Figure 6(b) demonstrates that decreasing the emittance above the cutoff wavelength (δ_l^e) is more effective in efficiency improvement, as compared with further optimizing emittance below cutoff wavelength (δ_h^e).

The aforementioned emitters are still far from ideal either in terms of optical performance or thermal stability. The problem lies in the challenge to fabricate a robust emitter on the hot side of the system, mostly due to the strict restrictions on thermal stability. One straightforward solution would be to improve the emission spectrum on the cold side, i.e., the PV cell. By adhering an optical filter to the cell, spectrum tuning could also be readily achieved. This filter naturally requires cooling, and the moderate temperature allows for the introduction of multiple optically ideal materials and structures. In 2016, Bierman *et al.* employed a tandem plasma–interference optical filter in their STPV system [Fig. 6(c)],[28] assembled on the PV cell by polydimethylsiloxane (PDMS). The PDMS is optically transparent, providing a strong and compact bonding between the cell and the filter. They improved their system efficiency from 3.2% to 6.8% through the addition of this specific configuration. However, their filter mostly aims at depressing the emission below the bandgap [Fig. 6(d)], and hence, still deviates from a perfect narrowband emitter.

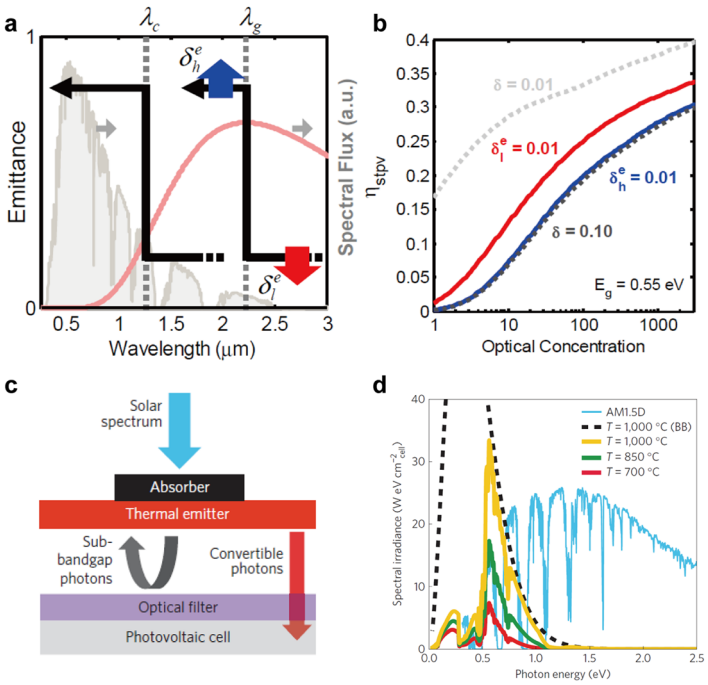

FIG. 6. Spectral nonidealities of the emitters and improvements by introducing filters. (a) Schematic of deviations from unity/zero emittance above/below the cutoff. (b) The impact of independently increasing/decreasing emittance below/above the cutoff wavelength of emitters. (c) Schematic of a filter enhanced STPV system. (d) Simulated spectral irradiances reaching the PV cell for different temperature. [(a) and (b)] Reprinted with permission from Lenert *et al.*, Opt. Express **22**(S6), A1604–A1618 (2014). Copyright 2014 OSA; [(c) and (d)] Bierman *et al.*, Nat. Energy **1**(6), 16068 (2016). Copyright 2016 Springer Nature.

IV. PV CELLS

A. Current status

In current STPV systems, low bandgap PV cells are chosen because of the relatively low temperature of the emitter. The major choices are III-V semiconductors, typically GaSb (0.7 eV),[29–31] InGaAs (0.6–0.7 eV),[32–34] and InGaAsSb (0.5–0.6 eV),[19] all of which are demonstrated with high light-to-electricity conversion performance. The fabrication technique for GaSb cells is mature as they were developed earlier, and the corresponding Zn diffusion technology has been well studied by research groups and companies.[35] InGaAs and InGaAsSb solar cells are fabricated by epitaxial technologies in laboratories and not yet commercialized, but the lower bandgap may enhance the system performance in the current operating temperature of emitters. Other cells suffer from inappropriate bandgaps or disappointing outputs. For example, InAsSbP cells are born with lower bandgaps (between 0.35 and 0.5 eV), but they are also equipped with a low open circuit voltage which undermines their overall efficiency.[36] Recently, researchers have been attempting to employ commercialized infrared detectors (InAs with 0.345 eV bandgap and InAsSb with 0.303 eV bandgap) as PV cells in their low temperature TPV experiments.[37] The external quantum efficiency (EQE) of these cells near the bandgap is usually below 0.4, but the system efficiency may be higher than those common TPV cells with lower emitter temperature.

The efficiency of the cell can be characterized by three factors, the ultimate efficiency, the voltage factor, and the fill factor. This was first systematically introduced by Shockley and Quiesser in their detailed balance model of solar cells,[1,3] where each photon with energy $h\nu$ greater than the bandgap energy $h\nu_g$ contributes to the electric power output $h\nu_g$. For a real solar cell, however, electricity is only contributed by photons with energy near the bandgap. As a result, quantum efficiency should be added into the formula for cell efficiency. Another difference from Shockley's model is that the input radiation is not the solar spectrum but the thermal emission of the emitter.

B. Optimizations of the optical response

Spectrum engineering on the PV cell is also of great importance, as conventional cells exhibit limited sub-bandgap reflectance and suffer from a great mismatch of the refractive index above the bandgap. Back surface reflectors (BSR) and antireflection coatings (ARC) are two main methods to overcome these problems. Here, the function of ARC is similar to that of the optical filters mentioned in Sec. III B, while enjoying the privilege of being well-cooled together with the PV cell. An ideal propagation of sub-bandgap photons includes passing through the ARC and active layer, being reflected by BSR, and returned to the emitter via the same path. Conclusions can be drawn from the above description that none of the layers are supposed to absorb sub-bandgap photons in the first place. Low-doped substrates are therefore recommended to reduce free carrier absorption. A layer of metal reflector is normally suggested for the design of BSR, which naturally shows limited sub-bandgap reflectance. Research by Burger *et al.* shows that an Au back surface reflector combined with a dielectric spacer layer can greatly enhance average sub-bandgap reflectance to 96%.[38] Such a design predicts a cell efficiency exceeding 50% via optical interaction with a 1500 K black emitter.

C. The matching of spectrum to bandgap

The temperature of the emitter determines the upper efficiency limit of the system. Meanwhile, to achieve a high power density, the emitter temperature should be high enough so that the blackbody peak matches the bandgap.[19] The peak depends on the description of the concrete mathematical form of the Planck's law. Interestingly, the peak of the solar spectrum is well-known in the visible region when plotted in wavelength units while shifted toward the near-infrared in frequency units.[39] This tricky difference originates from the fact that the radiation is described by a density distribution function in terms of the wavelength or frequency. A further contemplation at the calculation of cell efficiency, where one electron-hole pair excites per incoming photon, would lead us to the conclusion that neither the method is accurate for a precise calculation of the peak. Instead, the density distribution of photon numbers should be adopted due to a clearer physical interpretation. Figure 7 plots the aforementioned three types of spectra, where obviously the locations of the peaks are much varied for the same temperature of 1273 K. The proper bandgap, as extracted from Fig. 7(c), is 0.2 eV for such temperature. The bandgap of most frequently used

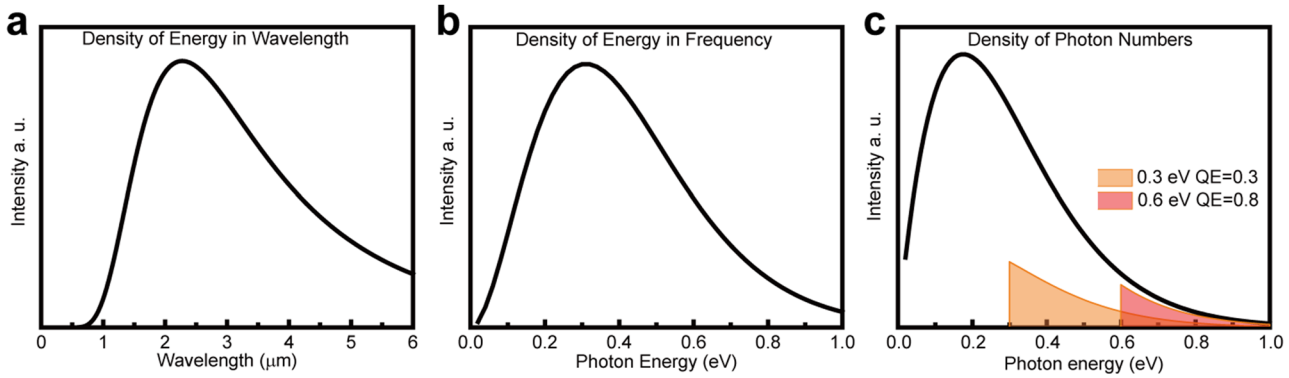

FIG. 7. Blackbody radiation spectrum of 1273 K described by (a) density of energy in units of wavelength, (b) density of energy in units of frequency, and (c) density of photon numbers. The orange and red area are the total numbers of effective photons for two different PV cells, a 0.3 eV bandgap cell with an average quantum efficiency of 0.3 and a 0.6 eV bandgap cell with an average quantum efficiency of 0.8.

narrow-band cells, however, ranges from 0.5 to 0.8 eV, making it difficult to maintain a high performance.

According to the photon density diagram, we can see that the commonly used narrowband cells such as InGaAs, InGaAsSb, and GaSb cells are not suitable for current operating temperature of STPV devices due to their large bandgaps. Some commercial infrared detectors (bandgap below 0.5 eV), despite a relatively low EQE, may be a better choice. As a demonstration, we have calculated the effective photon numbers for two cells at 1273 K, respectively; a 0.3 eV cell with average EQE of 0.3 (represents a InAsSb infrared detector) and a 0.6 eV cell with average EQE of 0.8 (represents a InGaAs cell). The effective photon numbers can be calculated as

$$N_{eff} = I_n(E) \cdot \eta, \tag{3}$$

where N_{eff} is the effective photon numbers, $I_n(E)$ is the intensity of the photon number at photon energy of E, η is the average EQE. As is shown in Fig. 7(c), 0.3 eV cell processes a larger area in the photon density diagram, indicating that the infrared detector, with a bandgap of 0.3 eV, can be utilized as a PV cell with better performance than commonly used cells in the STPV system.

Theoretically, high system efficiency can be achieved without the match of the spectrum peak to the bandgap of the cell, as the match only aims at high power density. In practice, however, a relatively high power density is beneficial to reducing the percentage of some parasitic losses, thereby improving the efficiency.

V. NONIDEALITIES BETWEEN STPV COMPONENTS

A. Absorber-to-emitter loss

The absorber and emitter are isothermal at the equilibrium temperature due to the high thermal conductivity of materials as well as their planar structures. Up until now, the energy transport from the absorber to the emitter is considered lossless. Experimentally, however, the holders or supports of the absorber and the emitter result in considerable conduction losses during the process. Needles are applied in recent works to support the sample for a reduction of conduction losses and a fin approximation is applied to calibrate this loss,[19] which is described as

$$\dot{q} = (T - T_v)\sqrt{h_n P k_n A}\tanh\left(\sqrt{\frac{h_n P}{k_n A}}L\right), \tag{4}$$

where T is the temperature at the contact of the sampler and needle, T_v the temperature of the system chamber, h_n the average heat transfer coefficient, P the perimeter, k_n the thermal conductivity, A the cross sectional area, and L the length of the needle. Needles are usually well-chosen metals with low thermal conductivity such as stainless steel. Ceramics, even with lower thermal conductivity, are not recommended, as they are too brittle to buffer the thermal expansion of the absorber and emitter.

B. Emitter-to-cell loss

In the radiative heat transfer process, a view factor means the proportion of the radiation which leaves one surface striking another. Herein, a view factor is introduced to exclusively evaluate the energy transfer efficiency from the emitter to the PV cell, due to their positive correlation [Fig. 8(b)]. In various experiments, researchers placed their emitter and PV cell largely adjacent to each other (approximately hundreds of microns) and claimed a view factor of unity in their efficiency analysis. In such a microscale dimension, however, the lost radiative energy still takes up a considerable proportion. In the course of seeking maximization of the view factor, five methods gradually emerged: reflectors around the emitter and cell, angular-selective emitters, near-field radiation systems, configuration engineering, and radiation guidance.

1. Reflectors around the emitter and cell

An inclusion of reflectors would efficiently recycle the escaped photons.[40] Figure 8 shows the importance of the view factor between tungsten emitters and filters. Figure 8(c) presents the theoretical modeling of the effect of an inserted side reflector between a 2800 K gray emitter and filter. The efficiency is defined as energy of the visible light transmitted through the filter [Fig. 8(a)], divided by the total energy radiated by the emitter. The radiative heat transfer is affected not only by the gap distance but also by the geometry of the emitter and filter, leading to a definition of a dimensionless parameter S^* referring to the ratio of gap spacing to the length

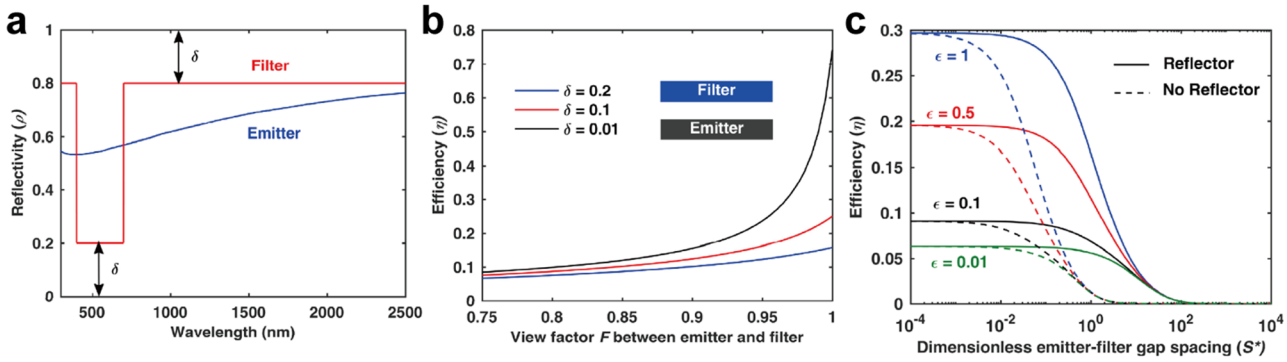

FIG. 8. An enhanced view factor via the inclusion of side reflectors. (a) Optical properties of a tungsten emitter and filter. (b) Efficiency of different emitter and filter systems. (c) Efficiency for different gray emitters with and without sider reflectors. Reprinted with permission from Leroy *et al.*, Opt. Express **26**(10), A462 (2018). Copyright 2014 OSA.

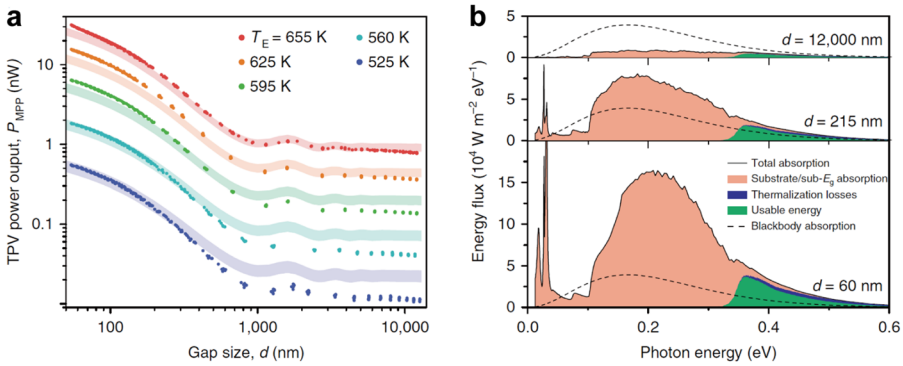

FIG. 9. The performance of a near-field STPV device. (a) Measured electrical output power (P_{MPP}) from 525 K to 655 K. (b) Calculated spectral energy flux for an emitter temperature of 655 K with different gap sizes *d*. Reprinted with permission from Fiorino *et al.*, Nat. Nanotechnol. **13**(9), 806–811 (2018). Copyright 2018 Springer Nature.

of the emitter. The authors also experimentally proved the theory by examining the power consumption of a tungsten emitter coupled with filters at different gaps with and without side reflectors. They witnessed over 10% reduction of power consumption at a 500 μm gap distance, with the inclusion of reflectors. These results are encouraging for its practical application in the STPV system.

2. Angular-selective emitters

Simply put, some multilayer structures can be tailored as angular selective emitters, since their interference effect is strongly affected by the incident angle. Sakr and Bermel proposed a design where an epsilon-near-zero thin film is backed by a metal reflector, covered with a high contrast grating, and combined with an angular selective transmission filter.[41] The high contrast grating couples guided modes to the thin film, the angular width of which is controlled by the period of grating. Angular selective filters are used to filter out off-directional modes, enhancing frequency selectivity. Directional emitters are considered a perfect way to enhance the view factor between emitters and cells, without extra attachments or reduction of gap distances. But current designs are mostly too complex to fabricate, which, along with the inherent instability, severely compromises their practicability.

3. Near-field radiation systems

When the gap is reduced to hundreds of nanometers or less, the energy transmission breaks the traditional Planck's radiation law.[42] Near-field radiation is therefore claimed to possess great potentials for the TPV energy conversion, in various computational studies.[43] Not until recently did Fiorino *et al.* design a near-field thermophotovoltaics device, which proved a ~40-fold enhancement in power output at 60 nm gaps as compared with far-field systems.[37] In their experiment, a silicon mesa on the suspended silicon beam is used as the emitter which can be heated to 655 K, and a commercial photodiode with a 0.345 eV bandgap energy is applied as the PV cell. It is seen that the output power rapidly increases as the gap reduces from 1000 nm to tens of nanometers [Fig. 9(a)]. The authors further calculated the energy flux spectrum from the emitter to the cell [Fig. 9(b)]. An over threefold enhancement of the blackbody radiation limit is observed due to the near-field effect. This work successfully demonstrated the construction of a near-field TPV system, but it is still far from a high-performance STPV system. With the temperature rising beyond 1000 K, the thermal management of PV cells becomes significantly difficult as the gap reduces to tens of nanometers. The almost linear current-voltage characteristic in the work indicates a low fill factor of the cell, implying a deleterious high operating temperature of the cell. This drawback may restrict the efficiency of the system to a large extent.

4. Configuration engineering

The planar structure is widely used in recent STPV works, and the exposure to the side shoulders the major responsibility of a low view factor. One solution is to construct an emitter-cell system with an omnidirectional coverage. Besides the radiation loss of the emitter, the system also suffers considerably from the radiation escape. One method is to build a PV cell cage encasing the absorber and the emitter.[44,45] In the cage-type system, the absorber/emitter absorbs the solar irradiance through the narrow aperture of the cell cage and transfers the captured broadband irradiance into a narrowband thermal emission, which omnidirectionally irradiates toward the surrounding PV cells. The absorbed photons can hardly escape the cage-type STPV because of the low leaking probability through the narrow aperture, ensuring high system efficiency. The systematic calculations by Wang *et al.* demonstrate that such a cage-type system can achieve a 10% improvement in efficiency.[45] It should be noted, though, that a hybrid absorber-emitter (HAE) is needed to ensure a highly useful radiation power of the system. Great efforts have been made to integrate these two components of broadband-absorption and narrowband-emission into one surface or structure, such as plasmonic structures and multilayer structures (Fig. 10).[44–47]

5. Radiation guidance

Through the guidance of radiation by total internal reflection between the emitter and the cell, this method is in fact similar with a reflector placed around the emitter and the cell. Zhou *et al.* calculated the effect of placing a photonic crystal waveguide between the emitter and a receiver, and proved a great improvement on the view factor.[48] The applied waveguide requires no cooling operations but is supposed to possess a low thermal conductivity. The obstacle of this design is still the high temperature instability of the materials and the structure; also, alignment of the waveguide between the emitter and the PV cell is difficult in practice.

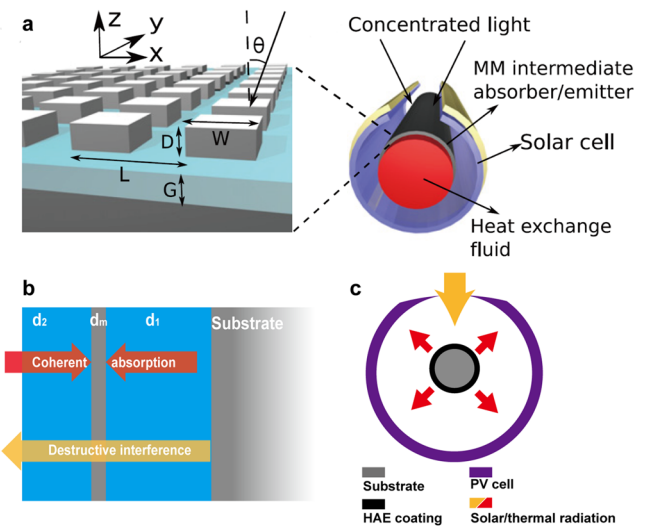

FIG. 10. Hybrid absorber-emitter (HAE) and STPV structure. [(a) and (b)] A plasmonic HAE and a pipe-type STPV system. Gray cubes indicate tungsten, and the blue film indicates Al_2O_3. [(c) and (d)] A multilayer HAE and the cross section of a cage-type STPV system. The gray layers indicate molybdenum, and the blue layers indicate HfO_2. [(a) and (b)] Reprinted with permission from Wu *et al.*, J. Opt. **14**(2), 024005 (2012). Copyright 2012 IOP Publishing; [(b) and (c)] Wang *et al.*, Adv. Opt. Mater. **6**(24), 1800813 (2018). Copyright 2018 WILEY-VCH.

VI. CONCEPTUAL EXTENSIONS OF STPV

With recent advances in STPV, exciting conceptual innovations are steadily popping out. The power source of the PV cell in STPV is not only thermal radiation but also other solar powered emission forms. Furthermore, a potential advantage of STPV is that it can continuous operating by using other heat sources or thermal storages. Here, we introduce few examples of them.

Thermophotonics (TPX): TPX is a system that incorporates light emitting diodes (LED) as emitters.[49,50] The LED emits photons higher than bandgaps of the PV cell, where the excess energy is supplied by a heat source such as the sun. If the LED is hotter than the PV cell, the extracted electric power can be higher than the energy injected into the LED. Compared with common STPV systems, the solar powered TPX allows for the employment of higher bandgap cells and with lower temperatures. The problem is also apparent: high performance LEDs with high temperature tolerances are not available so far, not to mention the fact that the external quantum efficiency of the LED should be near unity for high performance devices.

Solar pumped laser: Laser is a desirable energy source for PV cells, as it is directional, highly dense in energy, and has an extremely narrow band. The common method to pump a laser is through electric currents or light. Researchers have already demonstrated solar pumped lasers using a blackbody cavity.[51–54] The well-matched spectrum and the parallel direction of transmission both make the radiation loss comparably small, enabling a high performance of solar-to-electric energy conversion. However, heat to laser conversion efficiency is still low for now.

The hybrid system of solar TPV and fuel TPV: The concept derives from the use of the hybrid absorber-emitter (HAE).[45] The unique advantage of the one-side bifunctional structure renders the other side of the HAE ideal for the integration of STPV and TPV systems. A fuel tunnel can then be directly attached to the heated fluid, enabling an all-climate STPV system. With abundant sunshine, the HAE absorbs concentrated sunlight as normal and radiates the desired narrowband thermal emission to the surrounding PV cells. Meanwhile, the extra heat can be stored by the underlying energy storage materials; when sunlight is not available, the heated fluid in the tunnel provides thermal energy to the HAE, driving the operation of the TPV system as the alternative power source. The HAE-based all-climate STPV-TPV system can provide a competitive power supply solution to the nonideal environments and emergency situations such as a peak load of the grid, etc.

The hybrid system of STPV and thermoelectric generator: In the current STPV system, the PV cell is exposed under a high density thermal radiation, calling for a cooling attachment. The temperature could be very high as the gap between the emitter and the cell is reduced to hundreds of microns, as illustrated before. Attaching a thermoelectric generator on the back of the cell can successfully recycle the wasted energy. The risk is a potential enhancement in the temperature of the cell. A careful design is hence required to balance the temperature and the efficiency of the thermoelectric generator.

VII. OPPORTUNITIES

In summary, STPV holds promises for its high theoretical efficiency up to 85.4%, despite the yet unsatisfying experimental achievements. Future research into STPV technologies in materials and structures is expected to construct an efficient and cost-effective STPV system for industrialization and commercialization.

(1) Efficiency improvement: A rise in the operating temperature of absorbers and emitters up to 2544 K, from ~1500 K as in most configurations, is advantageous for achieving maximum efficiency as illustrated by Fig. 1. Higher solar concentration and lower conduction losses of sample holders are known to help increase the temperature. Narrowband emitters are also beneficial for heat conservation, besides its spectrum manipulation ability to improve efficiency. There is also a lot of room for the improvement of radiation transfer efficiency between components, such as the addition of side reflectors, the introduction of near-field radiation, etc.

(2) Materials' choice: For absorbers and emitters, long-term thermal stability should be guaranteed when the temperature is more than 1000 K. Their *in situ* optical performance at the operating environment is also understandably fundamental, which is nevertheless rarely measured or reported. These thermal properties are indisputably narrowing the choice of materials. For PV cells, those with a typical bandgap energy of 0.5–0.8 eV is investigated more instead of the more theoretically efficient low bandgap cells at relative low temperatures. Such cells as InAs and InAsSb cells are supposed to be promoted to enable a better performance at an operating temperature near 1200 K.

(3) Structural design: Typical planar-type STPV systems are easy to fabricate yet susceptible to multiple thermal losses, a challenge that the aforementioned cage structure and hybrid systems lead to a large extent resolve. These initiatives aim at the

efficiency enhancement and function extension separately, and an experimental establishment based on them is highly expected. Scale-up devices are also reported achieving a much higher system efficiency theoretically,[13] as the parasitic losses become relatively lower.

(4) Cost reduction: Current devices usually integrate vacuum systems and cooling systems, which increases the difficulty and the cost of system establishment, on top of the inevitable energy transfer loss. Researchers have attempted to create an inert gas chamber, injecting low heat capacity gases such as argon, to host the high-temperature absorbers and emitters.[26] Air-cooled heat sinks are also suggested to replace the forced liquid convection cooling system. More efforts can be made to reduce the indispensability of the above two systems.

ACKNOWLEDGMENTS

We acknowledge the microfabrication center of the National Laboratory of Solid State Microstructures (NLSSM) for technical support and the Jiangsu Donghai Silicon Industry Science and Technology Innovation Center. This work was jointly supported by the National Key Research and Development Program of China (Grant No. 2017YFA0205700), the State Key Program for Basic Research of China (Grant No. 2015CB659300), the National Natural Science Foundation of China (Grant Nos. 11874211, 11574143, 21805132, 11621091, and 61735008), the Natural Science Foundation of Jiangsu Province (Grant No. BK20180341), and the Fundamental Research Funds for the Central Universities (Grant Nos. 021314380140 and 021314380150).

REFERENCES

[1] W. Shockley and H. J. Queisser, J. Appl. Phys. **32**(3), 510–519 (1961).
[2] L. C. Hirst and N. J. Ekins-Daukes, Prog. Photovoltaics **19**(3), 286–293 (2011).
[3] E. Rephaeli and S. Fan, Opt. Express **17**(17), 15145–15159 (2009).
[4] S. Buddhiraju, P. Santhanam, and S. Fan, Proc. Natl. Acad. Sci. U. S. A. **115**(16), E3609–E3615 (2018).
[5] M. A. Green, *Solar Cells: Operating Principles, Technology, and System Applications* (Prentice-Hall, Englewood Cliffs, London, 1982).
[6] A. Datas and C. Algora, Sol. Energy Mater. Sol. Cells **94**(12), 2137–2147 (2010).
[7] J. Li, B. Liu, and S. Shen, Phys. Rev. B **96**(7), 075413 (2017).
[8] S. Molesky, C. J. Dewalt, and Z. Jacob, Opt. Express **21**(S1), A96–A110 (2013).
[9] B. Liu, W. Gong, B. Yu, P. Li, and S. Shen, Nano Lett. **17**(2), 666–672 (2017).
[10] H. Ghasemi, G. Ni, A. M. Marconnet, J. Loomis, S. Yerci, N. Miljkovic, and G. Chen, Nat. Commun. **5**, 4449 (2014).
[11] L. Zhou, Y. L. Tan, J. Y. Wang, W. C. Xu, Y. Yuan, W. S. Cai, S. N. Zhu, and J. Zhu, Nat. Photonics **10**(6), 393–398 (2016).
[12] D. Kraemer, Q. Jie, K. McEnaney, F. Cao, W. S. Liu, L. A. Weinstein, J. Loomis, Z. F. Ren, and G. Chen, Nat. Energy **1**, 16153 (2016).
[13] V. Rinnerbauer, S. Ndao, Y. X. Yeng, W. R. Chan, J. J. Senkevich, J. D. Joannopoulos, M. Soljačić, and I. Celanovic, Energy Environ. Sci. **5**(10), 8815 (2012).
[14] F. Cao, K. McEnaney, G. Chen, and Z. Ren, Energy Environ. Sci. **7**(5), 1615 (2014).
[15] J. Moon, D. Lu, B. VanSaders, T. K. Kim, S. D. Kong, S. H. Jin, R. K. Chen, and Z. W. Liu, Nano Energy **8**, 238–246 (2014).
[16] M. Garín, D. Hernández, T. Trifonov, and R. Alcubilla, Sol. Energy Mater. Sol. Cells **134**, 22–28 (2015).
[17] P. Li, B. Liu, Y. Ni, K. K. Liew, J. Sze, S. Chen, and S. Shen, Adv. Mater. **27**(31), 4585–4591 (2015).
[18] Y. Wang, L. Zhou, Q. Zheng, H. Lu, Q. Gan, Z. Yu, and J. Zhu, Appl. Phys. Lett. **110**(20), 201108 (2017).
[19] A. Lenert, D. M. Bierman, Y. Nam, W. R. Chan, I. Celanović, M. Soljačić, and E. N. Wang, Nat. Nanotechnol. **9**(2), 126–130 (2014).
[20] V. Rinnerbauer, A. Lenert, D. M. Bierman, Y. X. Yeng, W. R. Chan, R. D. Geil, J. J. Senkevich, J. D. Joannopoulos, E. N. Wang, M. Soljačić, and I. Celanovic, Adv. Energy Mater. **4**(12), 1400334 (2014).
[21] X. Q. Li, W. C. Xu, M. Y. Tang, L. Zhou, B. Zhu, S. N. Zhu, and J. Zhu, Proc. Natl. Acad. Sci. U. S. A. **113**(49), 13953–13958 (2016).
[22] F. Cao, D. Kraemer, T. Sun, Y. Lan, G. Chen, and Z. Ren, Adv. Energy Mater. **5**(2), 1401042 (2015).
[23] A. Datas and C. Algora, Prog. Photovoltaics **21**(5), 1025–1039 (2013).
[24] M. Shimizu, A. Kohiyama, and H. Yugami, J. Photonics Energy **5**(1), 053099 (2015).
[25] A. Kohiyama, M. Shimizu, and H. Yugami, Appl. Phys. Express **9**(11), 112302 (2016).
[26] T. Bauer, *Thermophotovoltaics: Basic Principles and Critical Aspects of System Design* (Springer Science and Business Media, 2011).
[27] A. Lenert, Y. Nam, D. M. Bierman, and E. N. Wang, Opt. Express **22**(S6), A1604–A1618 (2014).
[28] D. M. Bierman, A. Lenert, W. R. Chan, B. Bhatia, I. Celanović, M. Soljačić, and E. N. Wang, Nat. Energy **1**(6), 16068 (2016).
[29] L. G. Ferguson and L. M. Fraas, Sol. Energy Mater. Sol. Cells **39**(1), 11–18 (1995).
[30] M. Mauk and V. Andreev, Semicond. Sci. Technol. **18**(5), S191 (2003).
[31] J. M. Borrego, E. Brown, P. Greiff, D. L. Huffaker, R. B. Laghumavarapu, J. Kim, and P. S. Dutta, J. Renewable Sustainable Energy **6**(1), 011207 (2014).
[32] D. M. Wilt, N. S. Fatemi, P. P. Jenkins, R. Hoffman, G. A. Landis, and R. K. Jain, paper presented at the Photovoltaic Specialists Conference, 1996, Conference Record of the Twenty Fifth IEEEs.
[33] M. Tan, S. Lu, L. Ji, Y. Zhu, and Z. Chen, Jpn. J. Appl. Phys., Part 1 **52**(11R), 116504 (2013).
[34] M. Tan, L. Ji, Y. Wu, P. Dai, Q. Wang, K. Li, T. Yu, Y. Yu, S. Lu, and H. Yang, Appl. Phys. Express **7**(9), 096601 (2014).
[35] L. Fraas and L. Minkin, AIP. Conf. Proc. **890**, 17–23 (2007).
[36] V. M. Andreev, AIP. Conf. Proc. **653**, 383–391 (2003).
[37] A. Fiorino, L. Zhu, D. Thompson, R. Mittapally, P. Reddy, and E. Meyhofer, Nat. Nanotechnol. **13**(9), 806–811 (2018).
[38] T. Burger, D. J. Fan, K. Lee, S. R. Forrest, and A. Lenert, ACS Photonics **5**(7), 2748–2754 (2018).
[39] B. H. Soffer and D. K. Lynch, Am. J. Phys. **67**(11), 946–953 (1999).
[40] A. Leroy, B. Bhatia, L. Zhao, and E. N. Wang, Opt. Express **26**(10), A462 (2018).
[41] E. Sakr and P. Bermel, Phys. Rev. Appl. **7**(4), 044020 (2017).
[42] B. Song, A. Fiorino, E. Meyhofer, and P. Reddy, AIP Adv. **5**(5), 053503 (2015).
[43] M. Laroche, R. Carminati, and J. J. Greffet, J. Appl. Phys. **100**(6), 063704 (2006).
[44] C. Wu, B. Neuner III, J. John, A. Milder, B. Zollars, S. Savoy, and G. Shvets, J. Opt. **14**(2), 024005 (2012).
[45] Y. Wang, L. Zhou, Y. Zhang, J. Yu, B. Huang, Y. Wang, Y. Lai, S. Zhu, and J. Zhu, Adv. Opt. Mater. **6**(24), 1800813 (2018).
[46] H. Wang, Q. Chen, L. Wen, S. Song, X. Hu, and G. Xu, Photonics Res. **3**(6), 329 (2015).
[47] S. Behera and J. Joseph, J. Appl. Phys. **122**(19), 193104 (2017).
[48] Z. Zhou, O. Yehia, and P. Bermel, J. Nanophotonics **10**(1), 016014 (2016).
[49] J. Oksanen and J. Tulkki, J. Appl. Phys. **107**(9), 093106 (2010).
[50] D. J. Farrell, H. Sodabanlu, Y. P. Wang, M. Sugiyama, and Y. Okada, Nat. Commun. **6**, 8685 (2015).
[51] B. F. Gordiets, L. I. Gudzenko, and V. Y. Panchenko, JETP Lett. **26**(3), 152–154 (1977); available at http://www.jetpletters.ac.ru/ps/1375/article_20840.pdf.
[52] R. J. Insuik and W. H. Christiansen, AIAA J. **22**(9), 1271–1274 (1984).
[53] S. Johnson, F. Kuppers, and S. Pau, Opt. Laser Technol. **47**, 194–198 (2013).
[54] D. W. Liang, C. R. Vistas, B. D. Tiburcio, and J. Almeida, Sol. Energy Mater. Sol. Cells **185**, 75–79 (2018).